VISTA Is an Immune Checkpoint Molecule for Human T Cells

J. Louise Lines[1,2], Eirini Pantazi[1,2], Justin Mak[1,2], Lorenzo F. Sempere[3], Li Wang[4], Samuel O'Connell[1,2], Sabrina Ceeraz[4], Arief A. Suriawinata[5], Shaofeng Yan[5], Marc S. Ernstoff[3], and Randolph Noelle[1,2,3]

Abstract

V-domain Ig suppressor of T cell activation (VISTA) is a potent negative regulator of T-cell function that is expressed on hematopoietic cells. VISTA levels are heightened within the tumor microenvironment, in which its blockade can enhance antitumor immune responses in mice. In humans, blockade of the related programmed cell death 1 (PD-1) pathway has shown great potential in clinical immunotherapy trials. Here, we report the structure of human VISTA and examine its function in lymphocyte negative regulation in cancer. VISTA is expressed predominantly within the hematopoietic compartment with highest expression within the myeloid lineage. VISTA-Ig suppressed proliferation of T cells but not B cells and blunted the production of T-cell cytokines and activation markers. Our results establish VISTA as a negative checkpoint regulator that suppresses T-cell activation, induces Foxp3 expression, and is highly expressed within the tumor microenvironment. By analogy to PD-1 and PD-L1 blockade, VISTA blockade may offer an immunotherapeutic strategy for human cancer. *Cancer Res; 74(7); 1924–32. ©2014 AACR.*

Introduction

Immune responses must be tightly controled to allow effective clearance of invading pathogens or cancerous cells, and yet maintain tolerance to self. This is exemplified by the "signal 1/signal 2" paradigm for T-cell activation (1). Antigen-specific signals from the T cell receptor (TCR) ζ–CD3 complex and CD4/8-p56lck provide the "signal 1" for T cells. Whether this results in activation or anergy of the T cell depends on signal strength, and the combination of positive and negative cosignals provided by coreceptors in the immunoglobulin (Ig) superfamily—"signal 2" (2).

Positive regulators are typified by the CD28 receptor, which interacts with CD80 and CD86 (B7-1 and B7-2), resulting in the recruitment of its intracellular immunoreceptor tyrosine-based activation motif (ITAM) into the immune synapse (3). Generally, phosphorylated ITAMs serve as docking sites for Syk family tyrosine kinases (e.g., ZAP-70 or Syk) that potentiate T-cell signaling for activation (4).

In contrast, negative regulators tend to recruit phosphatases (e.g., SHP-1/2 or PP2A) that limit T-cell activation. The most well-characterized receptors in this group are cytotoxic T-lymphocyte antigen 4 (CTLA-4) and programmed cell death 1 (PD-1; ref. 5). Expression of CTLA-4 is induced by TCR signaling, allowing interaction with CD80 and CD86 to counteract CD28 (3). PD-1 acts more peripherally, interacting with PD-L1 in tissue sites to moderate T-cell responses.

Negative checkpoint regulators have come to the forefront of cancer research with the concept that tumor cells can exploit them to oppose immune attack in "adaptive resistance." This is illustrated by the success of blocking monoclonal antibodies (mAb) to CTLA-4 and PD-1 or PD-L1 in enhancing protective antitumor immunity (6–9).

Ipilimumab, the human anti-CTLA-4 mAb, has been approved for treating advanced melanoma, although the clinical response rate was low (10). It has also undergone early phase trials for other cancers (11). However, consistent with the severe autoimmune phenotype in CTLA-4^{KO} mice, anti-CTLA-4 therapy was associated with immune-related toxicities in patients (12). MDX-1106, the human anti-PD-1 mAb, has also produced promising results in clinical trials (13, 8). Early results suggest that the toxicity profile of MDX-1106 seems better than ipilimumab, with a response rate that is at least as good in a number of solid cancers (8). However, no effects on tumor growth were observed in prostate cancer, colorectal cancer, or with tumors negative for PD-L1 (8), suggesting that there may be other negative checkpoint regulators that are impairing the development of protective antitumor immunity.

Recently, our laboratory and others described a novel negative checkpoint regulator designated V-domain Ig suppressor of T cell activation (VISTA; refs. 14, 15). VISTA shares homology to PD-L1, and like PD-L1, potently suppresses T-cell activation. In mice, VISTA is highly expressed on tumor-infiltrating leukocytes, and blockade enhances antitumor immunity in multiple tumor models (16).

In this article, we present the first studies on the structure, function, and expression of human VISTA. Our studies show

Authors' Affiliations: [1]Medical Research Council Centre of Transplantation, Guy's Hospital, King's College London, King's Health Partners; [2]Department of Immune Regulation and Intervention, King's College London, London, United Kingdom; [3]Department of Medicine, Geisel School of Medicine at Dartmouth; [4]Department of Microbiology and Immunology, Dartmouth Medical School; and [5]Department of Pathology, Dartmouth-Hitchcock Medical Center, Lebanon, New Hampshire

Note: Supplementary data for this article are available at Cancer Research Online (http://cancerres.aacrjournals.org/).

Corresponding Author: J.L. Lines, King's College London, Guy's Hospital, London SE1 9RT, United Kingdom. Phone: 020-7188-1525; Fax: 020-7188-5660; E-mail: janet.lines@kcl.ac.uk

doi: 10.1158/0008-5472.CAN-13-1504

that human VISTA can profoundly suppress human T-cell activation, induce Foxp3, and we propose VISTA as a new target for cancer immunotherapy.

Materials and Methods

Quantitative real-time PCR

The TissueScan Human Normal cDNA Array (Origene) was used to provide template cDNA for 48 major human tissues. TaqMan gene expression assays containing FAM dye-labeled TaqMan MGB probe were used for human VISTA (Hs00735289_m1) and PD-L1 (Hs01125301_m1) in multiplex with primer-limited assays for glyceraldehyde-3-phosphate dehydrogenase (GAPDH) endogenous control containing VIC/MGB probes. Ten-fold dilution series of these assays on monocyte cDNA showed no alteration in efficiency with assays performed in single-plex versus duplex. Real-time quantification was performed using TaqMan gene expression master mix on a Bio-Rad CFX96 optical reaction module on a C1000 thermal cycler. Data were analyzed using CFX Manager Software (Bio-Rad).

Production of VISTA–Ig fusion protein

A fusion protein was created consisting of amino acids (aa) 16–194 from the extracellular IgV domain of human VISTA and a form of human immunoglobulin G1 (IgG1) mutated for low binding of Fc receptors. The VISTA sequence was cloned into the SpeI–BamHI sites of the vector CDM7B (17). Protein was produced by transient transfection of Freestyle CHO cells using Freestyle transfection reagent and protein-free Freestyle Expression Media according to the manufacturer's instructions (Life Technologies). Supernatant was harvested after 5 days of growth and purified using standard protein G agarose column affinity purification (Roche). Protein was concentrated using 10K MWCO spin columns (Amicon).

Generation of anti-VISTA mAbs

Female C57BL/6 mice were immunized with human VISTA–Ig fusion protein emulsified in complete Freund's adjuvant (CFA). They were boosted 4 weeks later with protein in incomplete Freund's adjuvant (IFA), then 6 weeks later, with A20 cells overexpressing VISTA-red fluorescent protein. Finally, they were boosted with VISTA–Ig fusion protein without the adjuvant. Four days after this last boost, spleens from immunized mice were provided to APS Ltd. Hybridomas and antibodies were generated by APS Ltd. under contract. Hybridoma clones that produced VISTA-specific antibodies were selected after limiting dilution and screened by both ELISA and flow cytometry methods. In order to demonstrate specificity of the clone GA1, 10^6 peripheral blood mononuclear cells (PBMC) were stained with 5 μg/mL of GA1 in the presence of 10 μg of soluble VISTA–Ig. In addition, K562s were transfected with human VISTA and staining was compared with untransfected parent cells (Supplementary Fig. S1).

Cell preparation

Human apheresis samples were obtained from unidentified healthy human donors. To isolate PBMCs, blood was layered onto Lymphoprep (PAA) and isolated by density-gradient centrifugation. Interface cells were washed twice in PBS, then once in MACS buffer [PBS pH 7.4, 0.5% bovine serum albumin (BSA), 2mM EDTA] before undergoing magnetic bead selection with Miltenyi CD4 Negative selection Kit II, CD8 Negative Selection Kit, CD4 Memory T Cell Selection Kit, or the B Cell Isolation Kit II according to the manufacturer's instructions. For effector-cell isolation, CD4 T cells isolated with CD4 Negative Selection Kit II were subsequently depleted of $CD27^+$ cell types with Miltenyi CD27 positive selection beads.

Where indicated, before culture, T or B cells were labeled with 5-(and 6)-carboxyfluorescein diacetate succinimidyl ester (CFSE), as previously described (18). Briefly, labeling was performed by incubating cells at 10^6 cells per mL at 37°C for 10 minutes with 5 μmol/L CFSE in PBS containing 0.1% BSA. CFSE was quenched by adding twice the volume of complete media, followed by three washes in complete media.

Culture

For T-cell cultures, unless otherwise indicated, 96-well flat-bottomed plates were coated overnight with anti-CD3 (clone OKT3; BioXCell) at 2.5 μg/mL mixed together with 10 μg/mL (ratio 1:4) VISTA–Ig or control-Ig protein (110-HG; R&D Systems) in PBS at 4°C overnight. Wells were washed twice with RPMI 1640 before adding cells. T cells were plated at 2×10^5 cells per well in complete RPMI media (RPMI 1640, 10% heat-inactivated FBS, 1,000 U/mL penicillin, 1,000 μg/mL streptomycin, 50 μmol/L 2-mercaptoethanol, 2 mmol/L GlutaMAX; Life Technologies). When indicated, a titrated amount of anti-CD28 (clone 15E8; Miltenyi Biotech) or cytokines, interleukin (IL)-2, IL-4, IL-7, or IL-15 (Peprotech), was added to the cultured media. T-cell cultures were analyzed on day 2 for early activation markers, and on day 5 for late activation markers or CFSE profiles.

For B-cell cultures, flat-bottomed 96-well plates were coated with 10 μg/mL of VISTA–Ig or human recombinant Fc isotype control (R&D Systems). B cells were plated at 5×10^4 cells per well in complete Iscove's Modified Dulbecco's Media (IMDM; Life Technologies) with 10% human serum (Valley Biomedical), 1,000 U/mL penicillin, 1,000 μg/mL streptomycin, and 2 mmol/L glutamine (Life Technologies). B cells were stimulated with soluble *Kirin* CD40Agonist (clone 341G2ser-1) at 0.25 μg/mL for 4 days. They were then stained by flow cytometry to determine proliferation.

Flow cytometry

For staining the following culture, cells were harvested and transferred onto V-bottomed 96-well plates. Cells were washed with PBS and stained in violet (B cells) or near-infrared (T cells) fixable live-dead dye (Life Technologies) at room temperature for 30 minutes. Cells were washed with PBS and then stained with a cocktail of antibodies for T cells (CD4, CD8, and either CD25, CD69, or CD45RA; BD Biosciences) or B cells (CD19) in the presence of 1 μg/mL of human IgG for 20 minutes on ice. Cells were then washed twice in PBS, and resuspended in PBS for flow cytometry. Just before analysis, cells were filtered through a 40-μm nylon mesh.

For staining for VISTA expression, 10^6 PBMCs (prepared as in "Cell preparation") or 100 μL of whole blood was washed with FACS staining buffer (PBS/0.1% BSA/0.1% sodium azide) and then stained with antibodies for extracellular markers and 1 μg of human IgG. Antibodies against CD4, CD8, CD3, CD45RA, CD56, CD11b, CD11c, CD123, HLA-DR, CD14, CD16, and CD66b were purchased from BD Biosciences and anti-VISTA was produced in-house. To stain intranuclear Foxp3, we used the Foxp3 Fixation/Permeabilization Concentrate and Diluent Kit from eBioscience according to the manufacturer's directions but using anti-Foxp3 clone 236A/E7 from BD Biosciences.

Samples were acquired on a BD LSRFortessa cell analyzer (Becton and Dickinson) with FACSDiva software v6.2 (Becton and Dickinson) and analyzed with FlowJo software (Tree Star, Inc.). Graphs were created using graphed Prism 5 (GraphPad Software, Inc.).

Ethics

Studies were approved by National Health Service Hammersmith and Queen Charlotte's and Chelsea Research Ethics Committee (09/H0707/86).

Immunohistochemistry

We performed a fluorescence-based multiplex immunohistochemistry (IHC) assay, as previously described (19), with slight modifications in Leica Bond–automated staining station. Briefly, after heat-induced epitope retrieval in ER2 (Leica) for 20 minutes, protein expression of VISTA (clone GG8), CD8 (Leica), and CD11b (Abcam) was revealed in this order by sequential rounds of tyramide signal amplification reactions using anti-mouse (Bio-Rad), anti-mouse IgG2b (Santa Cruz Biotechnology), and anti-rabbit (Bio-Rad) horseradish peroxidase–conjugated secondary antibodies and tyramine-coupled fluorescein, rhodamine red, and dylight 594, respectively. In isotype control antibody slides, anti-VISTA antibody was substituted by an equal amount of normal mouse IgG1 (Santa Cruz Biotechnology). Consecutive 4 μm-thick formalin-fixed paraffin sections mounted on Leica Microsystems Plus Slides (code S21.2113.A) were used in these experiments. Deidentified tissue specimens were obtained from the Dartmouth Pathology Translational Research Program.

Results

The human VISTA protein

We previously published studies describing the structure and function of murine VISTA (14). A Basic Local Alignment Search Tool (BLAST) of the murine VISTA amino acid sequence against the human genome identifies chromosome 10 open reading frame 54 (C10orf54 or platelet receptor Gi24 precursor, GENE ID: 64115) with an e-value of 8e-165 and 77% identity. Common with murine VISTA, this protein is predicted to encode a type I transmembrane protein with a single extracellular IgV domain. Human VISTA is 311-aa long, consisting of a 32-aa signal peptide, a 130-aa extracellular IgV domain, 33-aa stalk region, 20-aa transmembrane domain, and a long 96-aa cytoplasmic tail.

VISTA expression analysis

The expression of VISTA in healthy human tissues was examined by real-time PCR analysis of a cDNA tissue panel (Origene; Supplementary Fig. S2A). Similar to mouse VISTA (14), human VISTA was predominantly, if not exclusively, expressed in hematopoietic tissues or in tissues that contain significant numbers of infiltrating leukocytes. This is suggestive of the importance of VISTA for immune-related functions. Interestingly, expression of VISTA was particularly high in human placenta, which may be indicative of a functional role for VISTA in allofetal tolerance. Although VISTA's closest homolog PD-L1 is expressed in peripheral tissues, it also shows this pattern of enrichment in placental and hematopoietic tissues (Supplementary Fig. S2B).

VISTA protein expression was also examined within the hematopoietic compartment by flow cytometry. PBMCs were isolated from peripheral blood and stained with the anti-VISTA mAb, GA1. The specificity of this clone in flow cytometry was confirmed by the ability of VISTA–Ig to block staining (Supplementary Fig. S1A). Furthermore, this antibody stained K562 cells transfected with human VISTA, but not the untransfected parental cell line (Supplementary Fig. S1B). VISTA was not expressed by B cells ($CD19^+$) or $CD56^{hi}$ NK cells, and was only observed on a small portion of $CD56^{lo}$ NK cells. However, approximately 20% of CD4 and CD8 T cells showed low density VISTA staining (Fig. 1A). Overall, VISTA was more highly expressed within the myeloid compartment. VISTA expression was observed within both of the "patrolling" ($CD14^{dim}CD16^+$) and "inflammatory" ($CD14^+CD16^{+/-}$) subsets of $CD11b^{hi}$ blood monocytes, and within both lymphoid $CD11c^{lo}$ $CD123^+HLA\text{-}DR^+$ and myeloid $CD11c^+CD123^{lo}HLA\text{-}DR^+$ subsets of dendritic cells. To examine the expression of VISTA within neutrophils ($CD66b^+CD11b^+CD14^-$), GA1 binding was determined within washed whole blood using CD14 monocytes as a positive control. $CD66b^+$ neutrophils were found to express VISTA, at an intermediate intensity, higher than T cells but lower than monocytes (Fig. 1B). In mice, it was reported that VISTA protein expression tracked with CD11b expression (14). It is of note therefore, that, as in mice, in human peripheral blood, VISTA is expressed on $CD11b^{hi}$ cells, but is low within $CD11b^{lo}$ cells (Fig. 1C).

The histologic expression of VISTA in human secondary lymphoid organs was evaluated by multiplex IHC using anti-VISTA mAbs. Expression in human spleen was predicted by real-time (RT)-PCR and flow cytometry analyses (not shown). We detected the expression of VISTA along with CD8 and CD11b using a fluorescence-based multiplex IHC assay (19) on normal splenic tissue. CD8 staining was used to define the T-cell zone of the spleen and CD11b as a marker of the myeloid lineage. The specificity of anti-VISTA mAbs was again confirmed by the ability of VISTA–Ig to block staining (Supplementary Fig. S1C). High levels of VISTA expression were observed in a large proportion of CD11b-expressing cells in the marginal zone (Fig. 1D). This is consistent with the finding by flow cytometry that the $CD11b^{hi}$ subset of myeloid cells expresses high densities of the VISTA protein. The lower intensity VISTA expression of lymphoid cells such as T cells in the periarteriolar lymphoid sheath was not readily detected by IHC.

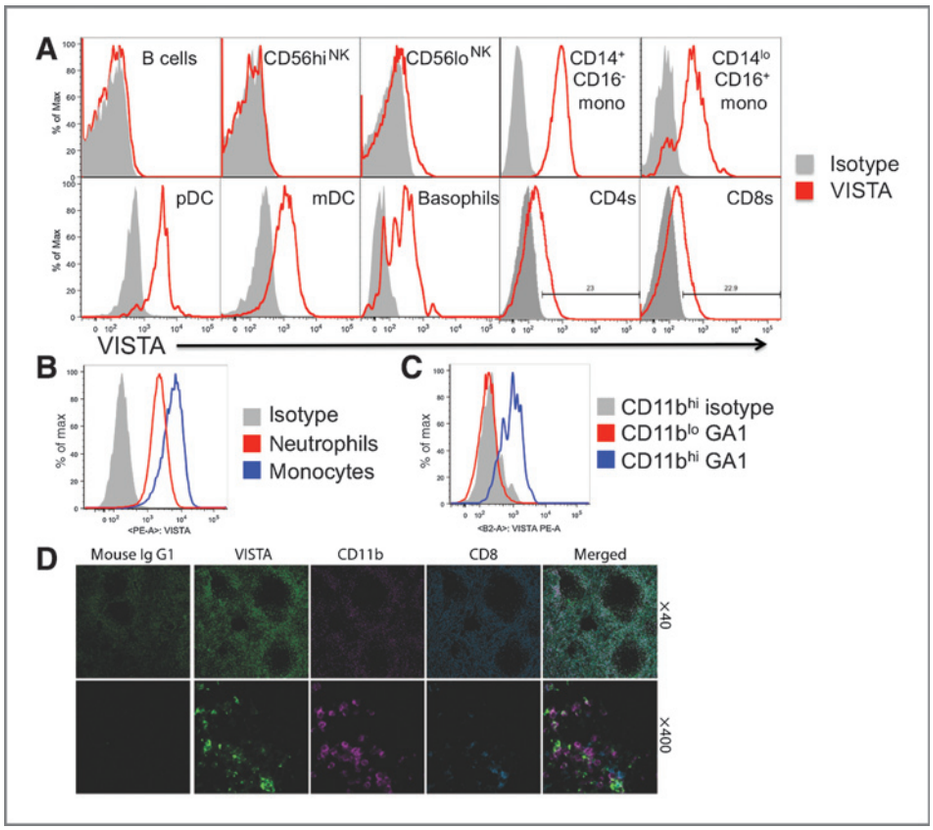

Figure 1. VISTA protein is predominantly expressed in the myeloid lineage within peripheral blood and normal spleen. Human PBMCs (A and C) or whole blood (B) were stained for VISTA expression. Overlays show representative overlays of VISTA (red) or isotype control (gray) live singlet-gated events from at least three independently stained donors. D, expression of VISTA, CD8, and CD11b was codetected in formalin-fixed paraffin-embedded sections of normal human spleen. In merged image panels, colocalization of VISTA (green) and CD11b (magenta) signal seems white. A consecutive tissue slide was stained with isotype control antibody (mouse IgG1; green). Original magnification of images was ×40 and ×400. Data are representative of four different donors.

Functional effect of VISTA on T-cell function

VISTA has previously been demonstrated to suppress mouse T-cell immune responses (14), and therefore a comprehensive set of studies with recombinant human VISTA was performed on a spectrum of human T-cell subsets to evaluate its suppressive activities. To this end, an Ig fusion protein was engineered, consisting of the extracellular domain of VISTA and the Fc region of human IgG containing mutations for reduced Fc receptor binding. VISTA–Ig or control-Ig was immobilized on plates with anti-CD3 (OKT3) and the ability of VISTA to suppress anti-CD3–induced T-cell proliferation was assessed by CFSE dilution. VISTA was found to suppress anti-CD3–induced CFSE dilution of bulk purified CD4 and CD8 T cells (Fig. 2A and B). The suppression by VISTA is comparable

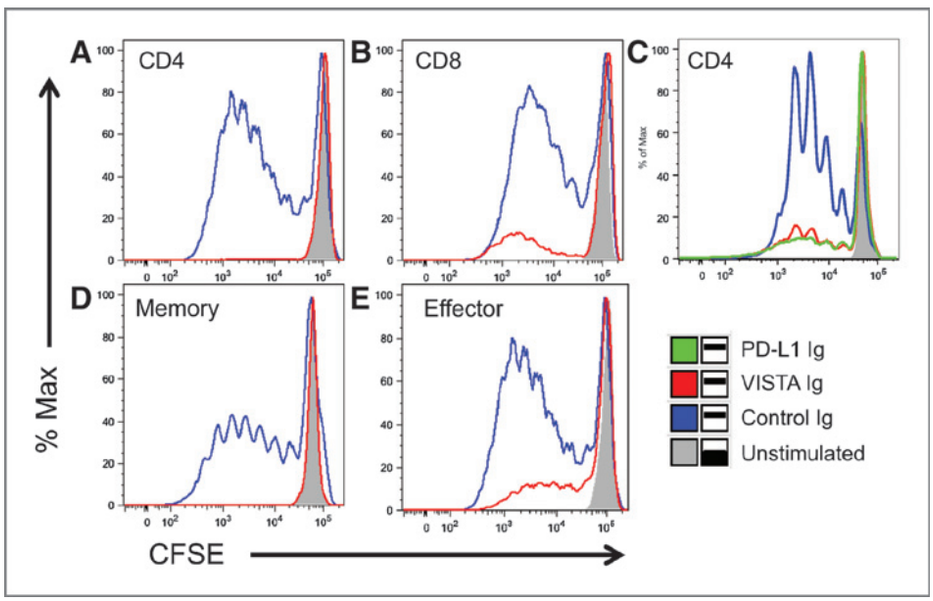

Figure 2. VISTA is suppressive to human T cells. Bulk CD4 (A and C), bulk CD8 (B), memory CD4 (D), or effector CD4 (E) T cells were purified from human PBMCs by magnetic bead selection. Cells were labeled with CFSE and stimulated for 5 days with 2.5 ug/mL anti-CD3 cocoated with 10 μg/mL of control-Ig (blue), VISTA–Ig (red), or PD-L1–Ig (green, C). Unstimulated cells (gray) are included for comparison. Cells are gated on live, singlet cells that are CD4 (A, C, D, and E) or CD8 (B) positive. Data are representative of at least two separate experiments.

with that induced by PD-L1–Ig at similar plate coating densities (Fig. 2C). In addition, VISTA–Ig was effective in the suppression of memory ($CD45RO^+$; Fig. 2D) and effector ($CD27^-$; Fig. 2E) CD4 T-cell subsets. Comparison of mouse VISTA and human VISTA on human CD4 T cells demonstrated that VISTA is functionally suppressive across mouse and human species (Supplementary Fig. S3A and S3B). Titration of human and murine VISTA–Ig over different concentrations of anti-CD3 showed that the proliferation induced at higher concentrations of anti-CD3 could be suppressed by coimmobilization of higher concentrations of VISTA (Supplementary Fig. S3C and S3D).

To gain insight into the mechanism of suppression, the activation status of cells was examined following stimulation in the presence or absence of VISTA–Ig. During 2 days of culture, upregulation by anti-CD3 of the early activation markers CD25 and CD69 was blocked by VISTA–Ig (Fig. 3A and B). Similarly, after 5 days of culture, the shift from expression of CD45RA to CD45RO, indicative of antigen-experience was prevented (Fig. 3C). VISTA had no effect on cell viability as judged by the exclusion of vital dyes or annexin staining (data not shown), and therefore did not seem to induce apoptosis. Consistent with a block in proliferation, cells treated with VISTA–Ig had forward- and side-scatter profiles similar to

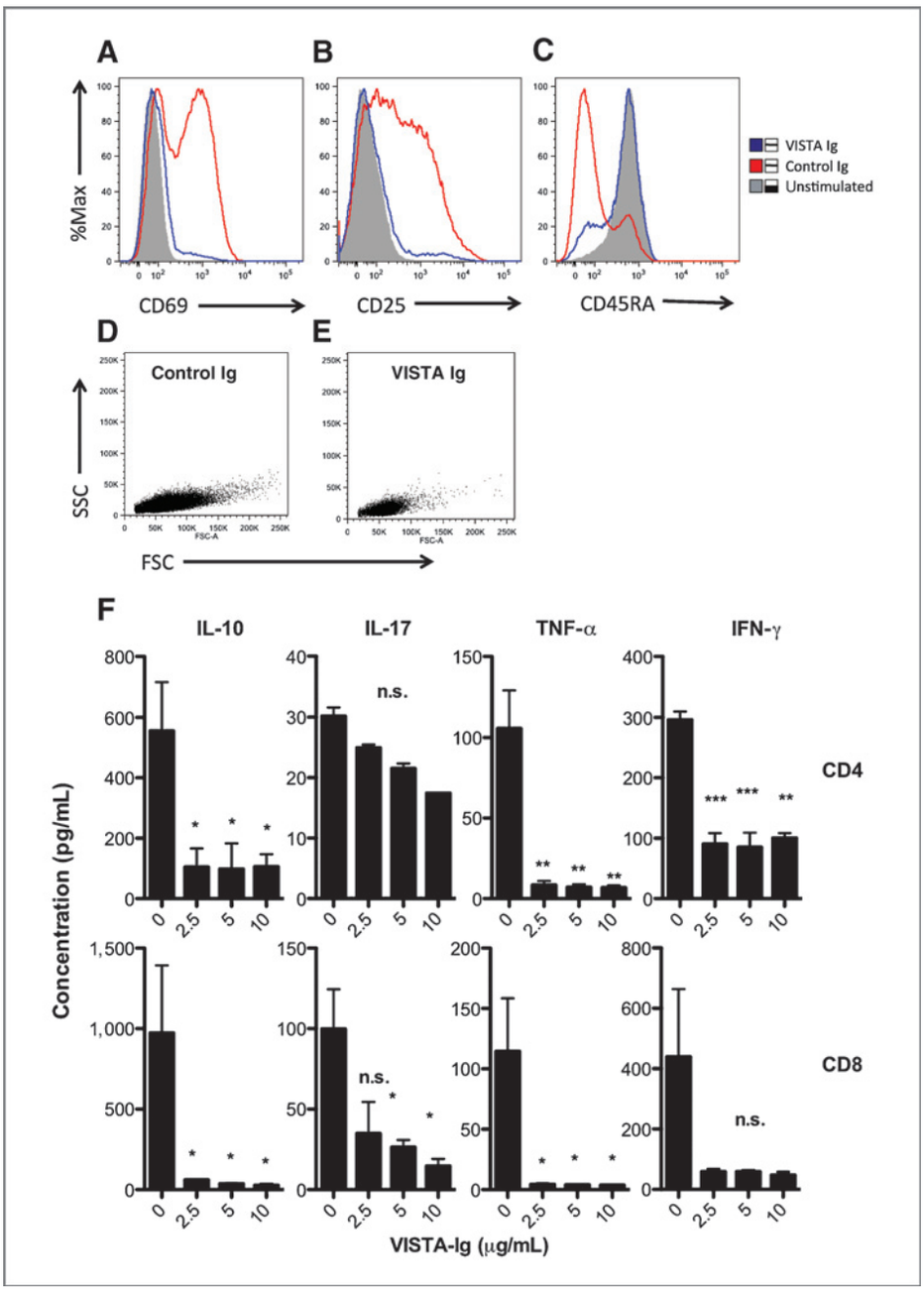

Figure 3. VISTA prevents anti-CD3–mediated induction of an activated T-cell phenotype. Bulk CD4 T cells were purified from human PBMCs by magnetic bead selection. Cells were stimulated for 2 (A and B) or 5 (C–F) days with 2.5 μg/mL anti-CD3 cocoated with 10 μg/mL of control-Ig (blue) or VISTA–Ig (red). Unstimulated cells (gray) are included for comparison. Cells are gated on live, singlet CD4 positive cells. F, the concentration of cytokines in the culture supernatant was determined by cytometric bead array and is shown as mean ± SD. *, $P < 0.05$; **, $P < 0.01$; ***, $P < 0.001$. Data are representative of at least two separate experiments.

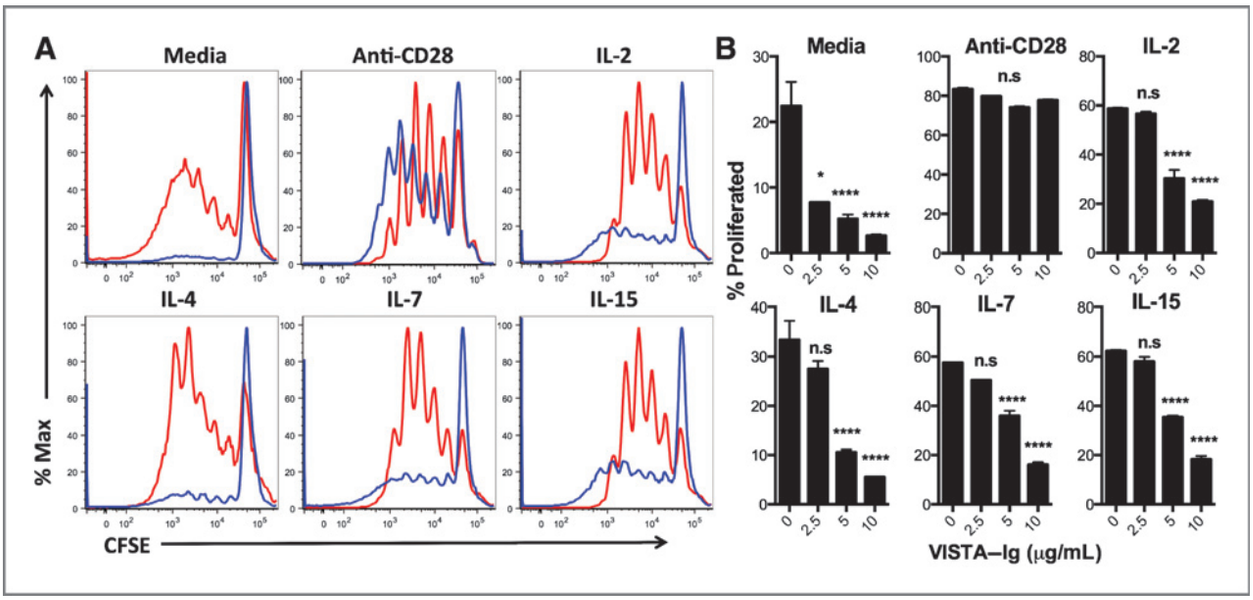

Figure 4. IL-7 family cytokines or CD28 costimulation can prevent the activity of lower concentrations of VISTA. Bulk CD4 T cells were purified from human PBMCs by magnetic bead selection. Cells were CFSE-labeled and stimulated for 5 days with 2.5 μg/mL anti-CD3 cocoated with VISTA–Ig or control-Ig in the presence of soluble factors in the culture media. A, 0, 250, 500, or 2,000 ng/mL of anti-CD28. B and C, 50 ng/mL of indicated cytokines. A and B, representative overlays showing 10 μg/mL control-Ig (red) and 10 μg/mL VISTA–Ig (blue). C, percentage CFSE low cells are shown as mean ± SD. Control-Ig was used to bring the concentration of fusion protein to 10 μg/mL in all wells. *, $P < 0.05$; **, $P < 0.01$; ***, $P < 0.001$. Data are representative of four separate experiments.

unstimulated cells rather than blasting cells seen with anti-CD3 alone (Fig. 3D and E). To determine if the suppression induced by VISTA is long-lasting, cells were cultured on anti-CD3 and VISTA–Ig for two days, and then viable cells were transferred onto anti-CD3–coated plates (in the absence of VISTA–Ig) for 3 days. This further stimulation was unable to rescue suppression as shown in Supplementary Fig. S4. Therefore, suppression of T-cell proliferation induced by VISTA is long-lasting, even in its absence.

The effect of VISTA–Ig on cytokine production was also evaluated. T cells were stimulated with plate-bound anti-CD3 for 5 days in the presence of increasing amounts of VISTA–Ig, and then the concentration of various cytokines was measured in culture supernatants by cytometric bead array. Only trace levels of IL-2, IL-4, or IL-6 were detected with anti-CD3 alone (<5 pg/mL), and no differences were observed when VISTA–Ig was also present (data not shown). However, VISTA–Ig significantly reduced the production of IL-10, TNF-α, and IFN-γ by CD4 and CD8 T cells (Fig. 3F), and there was a trend toward a modest decrease in IL-17 production.

Factors that were able to overcome VISTA-induced suppression of T cells were defined. Anti-CD28 agonistic antibody provides potent costimulation to T cells, and has been shown to overcome PD-L1–induced suppression of T cells. Titered concentrations of anti-CD28 were added into the cultures to address if VISTA-induced suppression could be reversed (Fig. 4). Although lower amounts of anti-CD28 were unable to overcome VISTA-induced suppression, when anti-CD28 was included at a coating concentration of 1 μg/mL VISTA–Ig, VISTA-Ig–induced suppression was reversed. On the other hand, even at supraphysiologic levels (50 ng/mL), the IL-2 family cytokines IL-2, IL-7, and IL-15 were only able to overcome a low concentration of VISTA-Ig (Fig. 4A and B).

As well as suppressing effector T-cell responses, PD-L1 is able to increase the conversion of naïve T cells into Foxp3$^+$ regulatory cells (regulatory T cells, Treg; refs. 20, 21). Under neutral culture conditions, VISTA–Ig ablates T-cell activation, which would prevent differentiation into Treg. Therefore, we examined Foxp3 expression after cultured at intermediate levels of anti-CD28 and IL-2 that still allowed some T-cell proliferation to occur. Under these conditions, conversion of naïve T cells into Foxp3 expressing T cells is significantly enhanced by the presence of VISTA–Ig (Fig. 5). As such, VISTA is both immunosuppressive and immunoregulatory.

Effect of VISTA on B cells

B cells were examined for their responsiveness to VISTA. To this end, B cells were isolated from human blood by immunomagnetic bead negative selection, and were cultured for 4 days in the presence of 250, 100, or 5 ng/mL of soluble CD40 agonist on 0, 1.25, 2.5, 5, or 10 μg/mL of VISTA–Ig or control-Ig. Proliferation was determined by CFSE dye dilution. As shown in Supplementary Fig. S5, immobilized VISTA–Ig was unable to suppress B-cell proliferation induced by CD40 signaling at high (10 μg/mL) concentrations (Supplementary Fig. S5A), even when the level of B-cell proliferation was titrated down by using low amounts of CD40 agonist (Supplementary Fig. S5B). Under the conditions used, VISTA–Ig has no impact on B-cell proliferation *in vitro*.

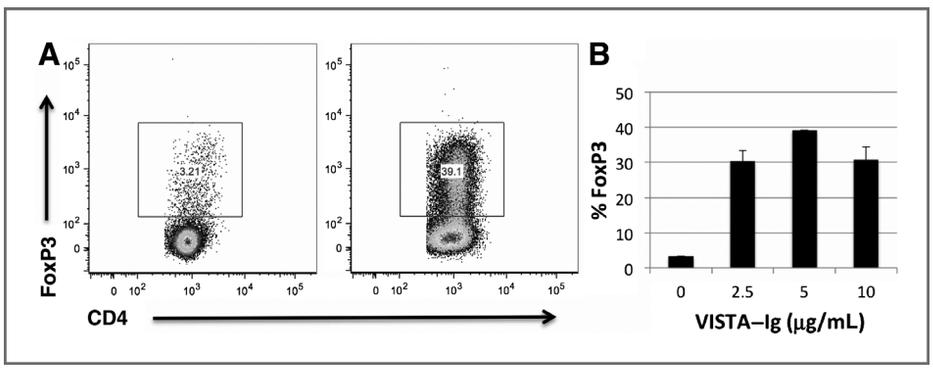

Figure 5. VISTA enhances conversion of human naïve T cells into Foxp3$^+$ T cells. Naïve CD4 T cells were purified from human PBMCs by magnetic bead selection. Cells were CFSE-labeled and stimulated for 5 days with 2.5 μg/mL anti-CD3 cocoated with VISTA–Ig or control-Ig in the presence of 10 ng/mL IL-2 and 250 ng/mL anti-CD28 in the culture media. A, representative plots showing Foxp3 within live, singlet CD4 T cells stimulated with 10 μg/mL control Ig (left) or 5 μg/mL VISTA–Ig and 5 μg/mL control Ig (right). B, percentage of Foxp3$^+$ cells is shown as mean ± SD. Control-Ig was used to bring the concentration of fusion protein to 10 μg/mL in all wells. Data are representative of three separate experiments.

Discussion

The studies presented are the first to describe the structure, function, and expression of human VISTA, a novel, hematopoietically expressed negative checkpoint regulator. Structurally, VISTA is a novel PD-L1–like ligand, with only one IgV domain and whose structure still is not fully resolved. Studies with a newly produced anti-human VISTA mAbs show that human VISTA is highly expressed on myeloid cells with reduced expression on CD4$^+$ and CD8$^+$ T cells. Functionally, human VISTA–Ig is profoundly suppressive on both resting and activated human CD4$^+$ and CD8$^+$ T cells. We propose VISTA as a promising new target for cancer immunotherapy, either as a single target or in combination with other immunotherapeutic strategies.

VISTA has an interesting expression pattern, with greatest mRNA detected in either hematopoietic tissues (i.e., spleen, lymph nodes, and peripheral blood) or those tissues with significant infiltration by leukocytes (Fig. 1). This suggests that VISTA is likely to have important immune functions. Overall, there is a good concordance between murine and human expression patterns for VISTA; however, human monocytes and myeloid lineage dendritic cells seem to uniformly express VISTA (Fig. 1A), whereas in mice, VISTA seems to track with the maturity of myeloid cells rather than be a characteristic of the myeloid lineage (14).

Notably, although T cells are responsive to VISTA, indicating that they express the receptor, T cells also express VISTA themselves (Fig. 1). This may be reflective of the function of VISTA. VISTA is expressed widely and sets a "danger" threshold that must be overcome before T cells become responsive. Although this may be counterintuitive, it may facilitate the maintenance of a quiescent state of naïve T cells as they receive tonic signals in T-cell zones of secondary lymphoid organs. In fact, expression of both ligand and receptor is not unique to VISTA. For example, PD-L1 is expressed on activated murine and human T cells, and particularly in mice, also on naïve T cells (22, 23). In addition to acting as a ligand for PD-1, PD-L1 has recently been shown to exert receptor function while interacting with CD80 (24, 25). PD-L1 therefore can signal bidirectionally from and to T cells. VISTA has a long cytoplasmic tail, and T-cell expression of VISTA may allow similar bidirectional signaling pathways on T cells.

Interestingly, mRNA for both PD-L1 and VISTA mRNA were found to be particularly high in human placenta (Supplementary Fig. S2). This is in agreement with studies showing high PD-L1 expression on placental trophoblasts and PD-L2 on placental decidual macrophages (26, 27), in which they play a critical role in maternal-fetal tolerance (28, 29). VISTA is most highly expressed on hematopoietic cells and in particular myeloid cells (Fig. 1). Given the rich blood supply of the placenta, and the presence of immunoregulatory macrophages, the prominent expression of VISTA is not unexpected. VISTA may contribute to the maintenance of maternal tolerance.

Both the work described herein (Figs. 2 and 3), and that of Wang and colleagues in mice (14), describe a profoundly suppressive role for VISTA toward T cells. As such, anti-VISTA mAb exacerbates experimental autoimmune encephalomyelitis (14) and enhances antitumor immune responses (submitted for publication). In fact, all of our data to date, both *in vivo* and *in vitro*, as well as preliminary studies in VISTA-deficient mice (unpublished data), clearly establish a negative regulatory role for VISTA. However, another study found that a mAb against VISTA prevents graft-versus-host disease in allogeneic mouse models, which is suggestive of a stimulatory role (15). At this time we cannot readily explain this discrepancy. Unique to this family, VISTA seems to be constitutively expressed on T cells, myeloid monocytic, and dendritic subsets (Fig. 1). In combination with a potentially constitutively expressed receptor, this suggests that VISTA exists as a negative regulator that must be overcome in order to initiate an immune response. Indeed, we found that strong costimulatory signals by anti-CD28 can overcome VISTA suppression (Fig. 4). Furthermore, the threshold can be adjusted by the activity of the γc family cytokines, so that the treated cells are less sensitive to VISTA (Fig. 4). These cytokines increase proliferation of T cells after antigen stimulation, and increased availability allows greater homeostatic proliferation (30). VISTA signals do shut down IL-2 production

(Fig. 3), however even supraphysiologic levels of γc family cytokines do not completely rescue VISTA-treated cells (Fig. 4), suggesting that VISTA does not exert its function through targeting the IL-2 pathway alone. It has been proposed that T cells require tonic signals through their TCRs from interaction with self-MHC to provide survival signals and maintain the size of the T-cell pool (31, 32). It is possible that VISTA may temper tonic T-cell signaling to prevent overt activation.

Clinical studies involving the use of antibodies that block negative checkpoint regulators, like CTLA-4, PD-1, and PD-L1 (33, 34), provide compelling evidence that these molecules impair the development of protective antitumor immunity. Furthermore, accumulating evidence suggests that expression of negative checkpoint regulators correlates with a poor patient outcome (35–39). The expression of these molecules within a given tumor microenvironment may vary widely from person to person, and the signature of checkpoint regulators may provide biomarkers for targeted treatment to achieve improved patient outcomes (40, 8). One particular advantage of VISTA as a therapeutic target may be its expression pattern. VISTA tends to be expressed on haematopoeitic cells rather than nonhematopoietic cells (Supplementary Fig. S2; ref. 14). In mouse tumors, infiltrating leukocytes such as myeloid-derived suppressor cells, tumor-associated macrophages and dendritic cells, consistently express unusually high levels of VISTA (submitted for publication), whereas nonhematopoietic tumor cells are negative. In contrast, PD-L1 is expressed in peripheral tissues and on tumor cells in areas of tumors with T-cell infiltration and expression of IFN-γ (41). Therefore, although the efficacy of PD-1 blockade seems to correlate somewhat with the expression of PD-L1 on the tumor (8, 41), the consistent expression of VISTA on leukocytes within the tumors may allow VISTA blockade to be more effective across a broad range of solid cancers. It could therefore be envisioned that blockade of different inhibitory molecules may be tailored to the individual. In this context, we envision that VISTA will be among the most relevant targets for immune intervention.

Development of treatments targeting VISTA would be much facilitated by knowledge of the receptor and its expression, and the receptor would also provide an additional target for antibody blockade. Structurally, VISTA is weakly related to the B7 family of proteins, which includes its closest homolog PD-L1. Immune regulatory proteins generally fall in either the Ig superfamily or the TNF superfamily (42). The majority of the B7 family interacts with CD28 family proteins in the Ig superfamily, with the notable exception of the negative checkpoint regulator B and T lymphocyte attenuator, which binds to Herpesvirus entry mediator, a TNF family member. We would predict that VISTA would also bind to a member of the Ig superfamily, but given the fact that VISTA has many unique structural features that separate it from the B7 family (14), it may have an unusual receptor. Interestingly, VISTA was recently demonstrated to bind the secreted protein bone morphogenetic protein 4 (BMP4; ref. 43). Although as a secreted protein this cannot be the receptor for transducing signals from VISTA–Ig, it is possible that BMP4 may modulate VISTA receptor function, or the receptor could even be in the BMP family. In any case, as an Ig-superfamily member expressed on the cell surface, it is expected that it will exhibit low-affinity interactions with fast dissociation rates (44, 45), and as such may be difficult to identify. We are actively pursuing multiple strategies to identify the receptor.

Disclosure of Potential Conflict of Interest

J.L. Lines is a consultant/advisory board member of ImmuNext. L.I. Wang has ownership interest (including patents) in ImmuNext and is a consultant/advisory board member of ImmuNext. S. O'Connell is a consultant of ImmuNext. R. Noelle is a CSO of ImmuNext and received commercial research grant from ImmuNext and has ownership interest (including patents) in ImmuNext. No potential conflicts of interest were disclosed by the other authors.

Disclaimer

The views expressed in this article are those of the author(s) and not necessarily those of the NHS, the National Institute for Health Research (NIHR), or the Department of Health.

Authors' Contributions

Conception and design: J.L. Lines, L. Wang, S. Yan, R. Noelle
Development of methodology: J.L. Lines, L.F. Sempere, L. Wang, S. O'Connell, S. Ceeraz, R. Noelle
Acquisition of data (provided animals, acquired and managed patients, provided facilities, etc.): J.L. Lines, L.F. Sempere, E. Pantazi, J. Mak, S. O'Connell, A.A. Suriawinata, S. Yan, M.S. Ernstoff
Analysis and interpretation of data (e.g., statistical analysis, biostatistics, computational analysis): J.L. Lines, L. Wang, E. Pantazi, S. O'Connell, M.S. Ernstoff, R. Noelle
Writing, review, and/or revision of the manuscript: J.L. Lines, L.F. Sempere, M.S. Ernstoff, R. Noelle
Administrative, technical, or material support (i.e., reporting or organizing data, constructing databases): J.L. Lines, E. Pantazi, S. O'Connell, S. Yan
Study supervision: L. Wang

Acknowledgments

The research was supported by the NIHR Biomedical Research Centre based at Guy's and St Thomas' NHS Foundation Trust and King's College London. The authors acknowledge tissue procurement and processing services from the Dartmouth-Hitchcock Pathology Translational Research Program.

Grant Support

This study was supported by AICR 12-1305 (R. Noelle and J. Lines), NIH R01AI098007, Wellcome Trust, Principal Research Fellowship (R. Noelle), R01CA164225 (L. Wang), and a Hitchcock Foundation pilot grant (L.F. Sempere).

The costs of publication of this article were defrayed in part by the payment of page charges. This article must therefore be hereby marked *advertisement* in accordance with 18 U.S.C. Section 1734 solely to indicate this fact.

Received May 28, 2013; revised November 15, 2013; accepted November 16, 2013; published online April 1, 2014.

References

1. Bretscher P, Cohn M. A theory of self-nonself discrimination. Science 1970;169:1042–9.
2. Sadegh-Nasseri S, Dalai SK, Korb Ferris LC, Mirshahidi S. Suboptimal engagement of the T-cell receptor by a variety of peptide–MHC ligands triggers T-cell anergy. Immunology 2010;129:1–7.
3. Rudd CE, Taylor A, Schneider H. CD28 and CTLA-4 coreceptor expression and signal transduction. Immunol Rev 2009;229:12–26.
4. Johnson SA, Pleiman CM, Pao L, Schneringer J, Hippen K, Cambier JC. Phosphorylated immunoreceptor signaling motifs (ITAMs) exhibit

unique abilities to bind and activate Lyn and Syk tyrosine kinases. J Immunol 1995;155:4596–603.
5. Dariavach P, Mattéi M-G, Golstein P, Lefranc M-P. Human Ig superfamily CTLA-4 gene: chromosomal localization and identity of protein sequence between murine and human CTLA-4 cytoplasmic domains. Eur J Immunol 1988;18:1901–5.
6. Wolchok JD, Weber JS, Maio M, Neyns B, Harmankaya K, Chin K, et al. Four-year survival rates for patients with metastatic melanoma who received ipilimumab in phase II clinical trials. Ann Oncol 2013;24:2174–80.
7. Callahan MK, Wolchok JD. At the bedside: CTLA-4- and PD-1-blocking antibodies in cancer immunotherapy. J Leukocyte Biol 2013;94:41–53.
8. Topalian SL, Hodi FS, Brahmer JR, Gettinger SN, Smith DC, McDermott DF, et al. Safety, activity, and immune correlates of anti–PD-1 antibody in cancer. New Engl J Med 2012;366:2443–54.
9. Brahmer JR, Tykodi SS, Chow LQM, Hwu W-J, Topalian SL, Hwu P, et al. Safety and activity of anti-PD-L1 antibody in patients with advanced cancer. New Engl J Med 2012;366:2455–65.
10. Hoos A, Ibrahim R, Korman A, Abdallah K, Berman D, Shahabi V, et al. Development of ipilimumab: contribution to a new paradigm for cancer immunotherapy. Semin Oncol 2010;37:533–46.
11. Calabro L, Danielli R, Sigalotti L, Maio M. Clinical studies with anti-CTLA-4 antibodies in non-melanoma indications. Semin Oncol 2010;37:460–7.
12. Attia P, Phan GQ, Maker AV, Robinson MR, Quezado MM, Yang JC, et al. Autoimmunity correlates with tumor regression in patients with metastatic melanoma treated with anti-cytotoxic T-lymphocyte antigen-4. J Clin Oncol 2005;23:6043–53.
13. Brahmer JR, Drake CG, Wollner I, Powderly JD, Picus J, Sharfman WH, et al. Phase I study of single-agent anti-programmed death-1 (MDX-1106) in refractory solid tumors: safety, clinical activity, pharmacodynamics, and immunologic correlates. J Clin Oncol 2010;28:3167–75.
14. Wang L, Rubinstein R, Lines J, Wasiuk A, Ahonen C, Guo Y, et al. VISTA, a novel mouse Ig-superfamily ligand that negatively regulates T cell responses. J Exp Med 2011;208:577–92.
15. Flies DB, Wang S, Xu H, Chen L. Cutting edge: a monoclonal antibody specific for the programmed death-1 homolog prevents graft-versus-host disease in mouse models. J Immunol 2011;187:1537–41.
16. Le Mercier I, Chen W, Lines JL, Day M, Li J, Sergent P, et al. VISTA Regulates the development of protective antitumor immunity. Cancer Res 2014;74:1933–44.
17. Hollenbaugh D, Douthwright J, McDonald V, Aruffo A. Cleavable CD40lg fusion proteins and the binding to sgp39. J Immunol Methods 1995;188:1–7.
18. Lyons AB. Analyzing cell division *in vivo* and *in vitro* using flow cytometric measurement of CFSE dye dilution. J Immunol Methods 2000;243:147–54.
19. Sempere LF PM, Yezefski T, Ouyang H, Suriawinata AA, Silahtaroglu A, Conejo-Garcia JR, et al. Fluorescence-based codetection with protein markers reveals distinct cellular compartments for altered microRNA expression in solid tumors. Clin Cancer Res. 2010;16:4246–55.
20. Wang L, Pino-Lagos K, de Vries VC, Guleria I, Sayegh MH, Noelle RJ. Programmed death 1 ligand signaling regulates the generation of adaptive Foxp3$^+$CD4$^+$regulatory T cells. P Natl Acad Sci U S A 2008;105:9331–6.
21. Francisco LM, Salinas VH, Brown KE, Vanguri VK, Freeman GJ, Kuchroo VK, et al. PD-L1 regulates the development, maintenance, and function of induced regulatory T cells. J Exp Med 2009;206:3015–29.
22. Yamazaki T, Akiba H, Iwai H, Matsuda H, Aoki M, Tanno Y, et al. Expression of programmed death 1 ligands by murine T cells and APC. J Immunol 2002;169:5538–45.
23. Greenwald RJ, Freeman GJ, Sharpe AH. The B7 family revisited. Annu Rev Immunol 2005;23:515–48.
24. Butte MJ, Peña-Cruz V, Kim M-J, Freeman GJ, Sharpe AH. Interaction of human PD-L1 and B7-1. Mol Immunol 2008;45:3567–72.
25. Butte MJ, Keir ME, Phamduy TB, Sharpe AH, Freeman GJ. Programmed death-1 ligand 1 interacts specifically with the B7-1 costimulatory molecule to inhibit T cell responses. Immunity 2007;27:111–22.
26. Petroff MG, Chen L, Phillips TA, Hunt JS. B7 family molecules: novel immunomodulators at the maternal-fetal interface. Placenta 2002;23:S95–S101.
27. Petroff MG, Chen L, Phillips TA, Azzola D, Sedlmayr P, Hunt JS. B7 family molecules are favorably positioned at the human maternal-fetal interface. Biol Reprod 2003;68:1496–504.
28. Taglauer ES, Trikhacheva AS, Slusser JG, Petroff MG. Expression and function of PDCD1 at the human maternal-fetal interface. Biol Reprod 2008;79:562–9.
29. Guleria I, Khosroshahi A, Ansari MJ, Habicht A, Azuma M, Yagita H, et al. A critical role for the programmed death ligand 1 in fetomaternal tolerance. J Exp Med 2005;202:231–7.
30. Rochman Y, Spolski R, Leonard WJ. New insights into the regulation of T cells by gamma(c) family cytokines. Nat Rev Immunol 2009;9:480–90.
31. Garbi N, Hämmerling GJ, Probst H-C, van den Broek M. Tonic T cell signalling and T cell tolerance as opposite effects of self-recognition on dendritic cells. Curr Opin Immunol 2010;22:601–8.
32. Hochweller K, Wabnitz GH, Samstag Y, Suffner J, Hämmerling GJ, Garbi N. Dendritic cells control T cell tonic signaling required for responsiveness to foreign antigen. P Natl Acad Sci U S A 2010;107:5931–6.
33. Wang S, Chen L. Immunobiology of cancer therapies targeting CD137 and B7-H1/PD-1 cosignal pathways. Curr Top Microbiol Immunol 2011;344:345–67.
34. Flies DB, Chen L. The new B7s: playing a pivotal role in tumor immunity. J Immunother 2007;30:251–60.
35. Gao Q, Wang X-Y, Qiu S-J, Yamato I, Sho M, Nakajima Y, et al. Overexpression of PD-L1 significantly associates with tumor aggressiveness and postoperative recurrence in human hepatocellular carcinoma. Clin Cancer Res 2009;15:971–9.
36. Inman BA, Sebo TJ, Frigola X, Dong H, Bergstralh EJ, Frank I, et al. PD-L1 (B7-H1) expression by urothelial carcinoma of the bladder and BCG-induced granulomata. Cancer 2007;109:1499–505.
37. Thompson RH, Gillett MD, Cheville JC, Lohse CM, Dong H, Webster WS, et al. Costimulatory B7-H1 in renal cell carcinoma patients: indicator of tumor aggressiveness and potential therapeutic target. P Natl Acad Sci U S A 2004;101:17174–9.
38. Nomi T, Sho M, Akahori T, Hamada K, Kubo A, Kanehiro H, et al. Clinical significance and therapeutic potential of the programmed death-1 ligand/programmed death-1 pathway in human pancreatic cancer. Clin Cancer Res 2007;13:2151–7.
39. Hamanishi J, Mandai M, Iwasaki M, Okazaki T, Tanaka Y, Yamaguchi K, et al. Programmed cell death 1 ligand 1 and tumor-infiltrating CD8+ T lymphocytes are prognostic factors of human ovarian cancer. P Natl Acad Sci USA 2007;104:3360–5.
40. Lu B, Chen L, Liu L, Zhu Y, Wu C, Jiang J, et al. T-cell-mediated tumor immune surveillance and expression of B7 co-inhibitory molecules in cancers of the upper gastrointestinal tract. Immunol Res 2011;50:269–75.
41. Taube JM, Anders RA, Young GD, Xu H, Sharma R, McMiller TL, et al. Colocalization of inflammatory response with B7-H1 expression in human melanocytic lesions supports an adaptive resistance mechanism of immune escape. Sci Transl Med 2012;4:127–37.
42. del Rio ML, Lucas CL, Buhler L, Rayat G, Rodriguez-Barbosa JI. HVEM/LIGHT/BTLA/CD160 cosignaling pathways as targets for immune regulation. J Leukoc Biol 2010;87:223–35.
43. Parisi S, Battista M, Musto A, Navarra A, Tarantino C, Russo T. A regulatory loop involving Dies1 and miR-125a controls BMP4 signaling in mouse embryonic stem cells. FASEB J 2012;26:3957–68.
44. van der Merwe PA, Barclay AN, Mason DW, Davies EA, Morgan BP, Tone M, et al. Human cell-adhesion molecule CD2 binds CD58 (LFA-3) with a very low affinity and an extremely fast dissociation rate but does not bind CD48 or CD59. Biochemistry 1994;33:10149–60.
45. van der Merwe PA, Neil Barclay A. Transient intercellular adhesion: the importance of weak protein-protein interactions. Trends Biochem Sci 1994;19:354–8.